(3) H. J. Howard and T. R. Lee, *Proc. Soc. Exp. Biol. Med.*, **24**, 700(1927).
(4) C. Trolle-Lassen, *Pharm. Weekbl.*, **93**, 148(1958).
(5) E. Friedman, *J. Amer. Med. Ass.*, **205**, 928(1968).
(6) W. T. Carpenter, *Arch. Ophthalmol.*, **78**, 445(1967).
(7) H. H. Mark, *J. Amer. Med. Ass.*, **186**, 430(1963).

ACKNOWLEDGMENTS AND ADDRESSES

Received March 23, 1970, from the *College of Pharmacy, University of Washington, Seattle, WA 98105*

Accepted for publication May 27, 1970.

This research was supported in part by Research Grant EY 00482 from the National Eye Institute, National Institutes of Health, Bethesda, Md.

Abstracted in part from a thesis submitted by Eunice S. N. Wang to the Graduate School, University of Washington, Seattle, Wash., in partial fulfillment of Master of Science degree requirements.

The authors wish to thank Dr. Carl Kupfer, Director, National Eye Institute, National Institutes of Health, formerly Chairman, Ophthalmology Department, University of Washington School of Medicine, for his help with the clinical portion of this investigation.

*To whom inquiries should be addressed.

Interactions of Drugs with Proteins II: Experimental Methods, Treatment of Experimental Data, and Thermodynamics of Binding Reactions of Thymoleptic Drugs and Model Dyes

H. J. WEDER* and M. H. BICKEL

Abstract □ The binding to bovine albumin of the model dyes and drugs—bromocresol green, eosin, imipramine, and desipramine—has been studied using equilibrium dialysis, ultracentrifuge sedimentation, and difference spectrophotometry. An improved apparatus for equilibrium dialysis has been developed. Bromocresol green interacts with two types of binding sites: four ligands are bound by H-bonds, electron-donator-acceptor (and possibly hydrophobic) forces stabilized by electrostatic forces, and three to four ligands are bound by electrostatic forces only. Eosin is bound by van der Waals' forces and electron-donator-acceptor forces to three binding sites and by electrostatic forces to six binding sites. Imipramine interacts with only one type of binding site by van der Waals' and possibly hydrophobic forces, stabilized by dipole-dipole forces and involving tyrosyl residues. There are $n = 6$ binding sites, and the intrinsic association constant $k = 5 \times 10^3$ M^{-1}. Desipramine binding exhibits a more complicated mechanism, probably involving exposure of additional binding sites upon a drug-induced conformational change. Given concentrations of drug and protein yield the free-drug concentration and degree of binding as experimental values. From these the following parameters for each type of binding site have been determined by computer: n, k, free-enthalpy change, enthalpy change, and entropy change. From these parameters, as well as from spectral shifts and dependence on pH, ionic strength, and temperature, the modes and forces of interaction have been deduced according to previously discussed binding models and methods. Identical results are obtained by dialysis and ultracentrifugation if pH, ionic strength, and temperature are kept constant.

Keyphrases □ Plasma protein-drugs—interactions □ Thymoleptics, dyes—bovine albumin binding □ Dyes, thymoleptics—thermodynamics, bovine serum binding □ Thermodynamics—drugs-albumin binding □ Dialysis, equilibrium—albumin binding □ UV spectrophotometry—analysis

It is generally assumed that a small molecule interacting with a biopolymer induces a conformational change which is responsible for the action of the small molecule (drug). Similar interactions or binding of drugs also occur with biopolymers not involved in pharmacological action, *i.e.*, with unspecific receptors such as plasma proteins.

The binding of a small molecule can influence the chemical reactivity at different sites of the macromolecule. These phenomena are mainly due to long-range electrostatic forces, to shorter range specific interactions such as hydrogen and hydrophobic bonds (1), and finally to proton dispersion forces; the latter obey the same laws as London dispersion forces (2). In addition, primary drug–protein complexes are often stabilized by charge transfer forces. These forces, however, should not be used to estimate the overall complex stability, since the interactions are mainly due to van der Waals–London forces. The stability of a drug–protein complex is expressed by its association constant, which is also important for the pharmacokinetic behavior of the drug.

Numerous methods are currently used for the study of drug–protein interactions (3). Thermodynamic methods and optical rotatory dispersion (ORD) or circular dichroism measurements are tools for the detection of drug-induced conformational changes of a biopolymer. Equilibrium dialysis and ultracentrifugation, as well as spectroscopy in the visible and UV range, allow the determination of association constants. The resulting energy and entropy effects are useful parameters for the interpretation of the mechanism of interaction. Difference spectra in the 220–310-mμ range yield information on conformational changes in the environment of phenylalanyl, tyrosyl, and tryptophyl residues. High resolution NMR spectroscopy is a powerful tool for the study of primary binding sites and of drug atoms interacting with the macromolecule. Information on the mobility of the interacting groups can, in this way, be obtained by the determination of relaxation times.

In this paper, the authors present the results of experiments with triphenylmethane dyes and bovine albumin designed to test methods used in the study of drug–protein interactions. Some of these methods were used in the earlier study of tricyclic thymoleptic drugs (4). This paper also contains additional data on the thermodynamics and binding mechanism of the drugs mentioned.

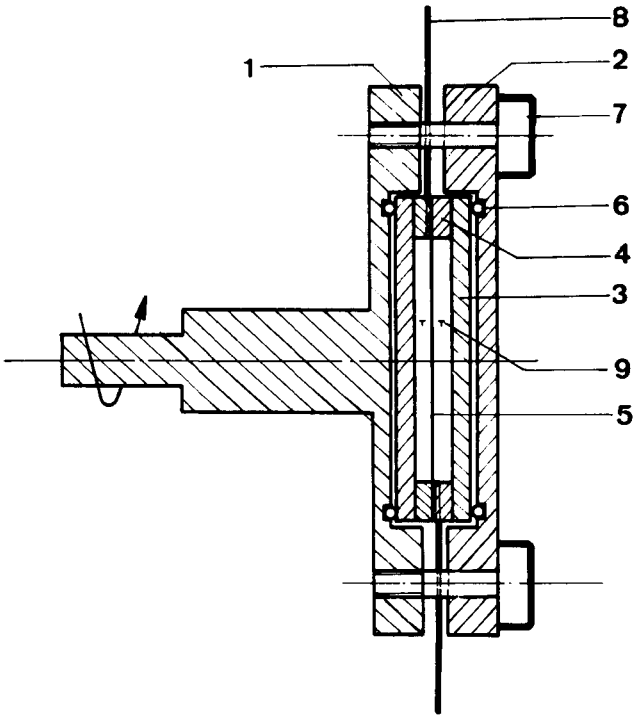

Figure 1—*Apparatus for equilibrium dialysis. Key: 1, Plexiglas core; 2, Plexiglas lid; 3, glass disk; 4, Teflon ring; 5, membrane; 6, rubber ring; 7, binding screw; 8, Cr–Ni tubes, 1.4-mm. diameter; and 9, surface of liquid in dialysis cells. For further details, see* Experimental.

EXPERIMENTAL

Materials—The purity of the dyes, bromocresol green (BKG) and eosin (EOS),[1] was checked by TLC. All other compounds used were described previously (4). The buffer solutions are indicated in the respective tables and figures.

Spectrophotometry—All measurements were carried out at 20 ± 2° with a Unicam UV spectrophotometer SP 800 and a 1-cm. cell. The following molar extinction coefficients have been determined for BKG (ϵ^{20}_{616}) and EOS (ϵ^{20}_{515}), respectively: 2.93×10^4 and 5.94×10^4 (pH 7.0 phosphate buffer, 0.01 *M*), 2.04×10^4 and 5.50×10^4 (pH 5.0 disodiumcitrate buffer, 0.05 *M*), and 1.32×10^4 and 3.26×10^4 (pH 3.5 citric acid–phosphate buffer 0.05 *M*). The relative errors were <3%.

To use a spectral change for the determination of the free and protein-bound dye, the following conditions must be fulfilled:

1. There is no absorbance of the protein in the spectral range used.
2. Free and bound ligands obey Beer's law in the concentration range used.
3. Extinction coefficient (ϵ) of bound ligand is independent of degree of binding (r).
4. There is the appearance of an isosbestic point ($\epsilon_{free} = \epsilon_{bound}$).

Calculations of association constants can be carried out according to Benesi and Hildebrand (6) or Hammes and Schimmel (7). The molar ratio of an interaction can be determined by extrapolation of the difference spectrophotometric titration curve at saturation ($r = n$) obtained by varying the concentration of either ligand or protein.

Equilibrium Dialysis—The fraction of a ligand bound to a protein can be determined by measuring the free ligand concentration in the protein-free compartment. Membrane effects can be controlled if the ligand concentration can be determined in both compartments. Under certain conditions (8), the Donnan effect must be corrected for (9, 10). The devices used for equilibrium dialysis range from simple cellophane bags (11–13) to specially designed apparatus (14, 15). The one developed by the authors contains two cells (3.0 ml., 0.27-cm. width), separated by a regenerated cellulose membrane of a medium pore size of 3–5 mμ and a weight of 12.8 g./m.^{2}. The vertically positioned wheel-shaped double cell is rotated at 100 r.p.m. Each cell contains two metal tubes in opposite position. They are used for filling and emptying the cells and are connected by a plastic tube during dialysis. Further details are shown in Fig. 1. The main advantages (14) of this device, as compared to others, are a constant solution volume (pressure compensation), minimal dilution effects, short equilibration times, and low risk of denaturation.

To suppress Donnan effects, the buffer solutions contained 0.9% NaCl. The dialyses were carried out at 20 ± 1 and 4 ± 1°, respectively. The experimentally determined equilibration times were in the 2–3 hr. range for all ligands used [imipramine (IP), desipramine (DMI), BKG, and EOS]. Addition of these ligands to the buffer cell or to the protein cell led to identical results. In the latter case, an incubation time of 30 min. was allowed before dialysis. The binding reactions have been found to be reversible. The weak adsorption of IP and DMI to the membrane has been controlled by measuring the equilibration concentrations in both cells. The concentrations were determined either by measurement of radioactivity (4) or spectrophotometry.

Ultracentrifugation—In a strong gravitational field, sedimentation of proteins and protein–ligand complexes can be obtained whereas the free ligand concentration remains unchanged. The method described by Steinberg and Schachman (16, 17) has been used.

Ultracentrifugation was carried out at 200,000 × *g* for 16 hr. at 21 ± 1°.

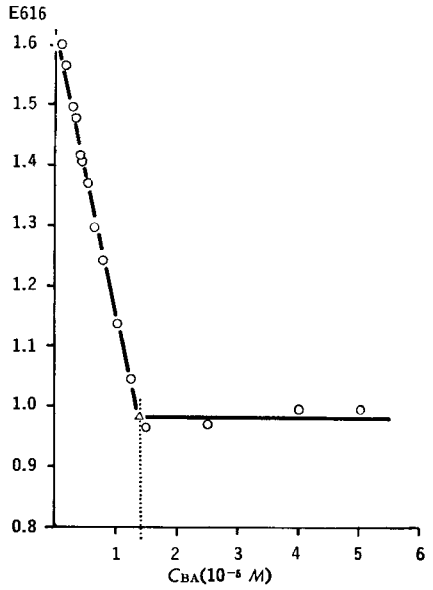

Figure 2—*BKG–BA interaction (pH 7.00). Saturation curve obtained by spectrophotometric titration. For further details, see* Results.

CALCULATION OF BINDING PARAMETERS

The basic theory of the calculation of ligand–protein equilibria has been described in detail (11, 13, 18, 19). In many cases, a clear interpretation of experimental data is hampered by the occurrence of more than one type of binding site, one or more interacting types of binding sites, or by cooperative binding phenomena. In certain cases, particularly when important chemical and physical characteristics of the macromolecule are known, the correction function, $f(r)$, can lead to the desired result (20).

Various curve-fitting techniques can be employed for the determination of the number of individual binding sites and association constants by solving a set of i simultaneous linear equations for a system of i binding types (21).

A graphic method, employed when the characteristics and concentration of the protein are unknown, has been described by Rosenthal (22), making it possible to determine the physicochemical parameters of binding systems which consist of one ligand and one or more proteins containing one or more noninteracting binding

[1] Purchased from Fluka Ltd., Buchs, Switzerland.

Table I—BKG–BA Interaction Showing Binding Parameters and Comparison of Methods at 21°

Method	pH	Ionic Strength	n_1[a]	n_2[a]	k_1,[b] 10^5 l./mole	k_2, 10^3 l./mole	$\Delta F_1°$,[c] cal./mole	$\Delta F_2°$, cal./mole
DIA[d]	7.0	0.19[e]	4.07 ± 0.18	3–4[f]	5.48 ± 0.25	—	−7718	—[f]
UCS[g]	7.0	0.19[e]	4.11 ± 0.21	3–4[f]	5.62 ± 0.34	—	−7732	—[f]
UCS	7.0	0.04[h]	4.19 ± 0.12	3–4[f]	13.2 ± 0.4	—	−8231	—[f]
TIT[i]	7.0	0.04[h]	3.6	—	—	—	—	—
UCS	5.0	0.24[j]	58 ± 2	44 ± 4	0.06 ± 0.03	1.31 ± 0.10	−4942	−4192
UCS	3.5	0.25[k]	108 ± 8	0	0.47 ± 0.04	0	−5113	0

[a] n = number of (primary and secondary) binding sites. [b] k = intrinsic association constant. [c] $\Delta F°$ = free-enthalpy change. [d] DIA = equilibrium dialysis. [e] Phosphate buffer, 0.01 *M* + NaCl, 0.9%. [f] See *Discussion*. [g] UCS = ultracentrifuge sedimentation. [h] Phosphate buffer, 0.01 *M*. [i] TIT = spectrophotometric titration. [j] Disodium citrate buffer, 0.05 *M*. [k] Citric acid–phosphate buffer, 0.05 *M*.

sites. This method also yields information about the distribution of the ligands on the different types of binding sites.

Equations for the characterization of pure hydrophobic interaction mechanisms between phenols (23) or polycyclic hydrocarbons (24) and proteins have been developed from the protein association constants and partition coefficients of the ligand in question. Crothers (25) developed a computational method for the calculation of binding isotherms for heterogeneous polymer systems.

Theoretical studies toward determination of the binding functions of ligands that interact with a polymerizing protein system have been carried out by Nichol *et al.* (26). According to these authors, pronounced sigmoidal binding curves, as in the case of allosteric systems, are to be expected.

RESULTS

BKG–Bovine Albumin (BA)—The binding equilibrium of BKG and BA was investigated using three methods: difference spectrophotometry, equilibrium dialysis, and sedimentation in the ultracentrifuge.

The spectrophotometric titration of 5×10^{-5} *M* BKG solutions in 0.01 *M* phosphate buffer, pH 7.0, with corresponding BA solutions (molar excess range of BKG 1 to 100) yielded at saturation a binding stoichiometry of BA–BKG = 1:3.6 (Fig. 2). Difference spectra, involving constant BA concentrations and variable BKG concentrations with corresponding BKG solutions as reference, show under like conditions absorption maxima at 413 and 632 mμ, the longwave red-shift maximum yielding the same stoichiometry (1:3.8). Since the absorption maxima of free BKG are 400 and 616 mμ, the charge transfer band of the albumin-bound BKG exhibits a shift of 13 and 16 mμ, respectively. At 616 mμ, a simultaneously appearing hypochromic effect of 32 ± 4% can be measured.

The evaluation of the experimental binding curves, as obtained by means of dialysis and ultracentrifugation, is based on the following model, which has also been successfully employed in the case of EOS–albumin interaction. This model assumes that the use of dilute solutions allows the activities of the components to be equated to their concentrations and, furthermore, that interactions between individual binding sites as well as cooperative binding phenomena are absent or negligible. If r is the mean degree of binding, *i.e.*, number of moles of bound ligand per mole of protein, and c_f the concentration in moles/liter of the free ligand at equilibrium, then

$$r = \sum_{i=1}^{i=q} \frac{n_i \cdot k_i \cdot c_f}{1 + k_i \cdot c_f} \qquad \text{(Eq. 1)}$$

where n_i represents the maximal number of the equivalent binding sites of q different types, and k_i is the corresponding intrinsic association constants. In the case of two types of binding sites, Eq. 1 becomes

$$r = \frac{n_1 \cdot k_1 \cdot c_f}{1 + k_1 \cdot c_f} + \frac{n_2 \cdot k_2 \cdot c_f}{1 + k_2 \cdot c_f} \qquad \text{(Eq. 2)}$$

or for one type of binding site,

$$r = \frac{n_1 \cdot k_1 \cdot c_f}{1 + k_1 \cdot c_f} \qquad \text{(Eq. 3)}$$

or

$$\frac{r}{c_f} = k_1 \cdot n_1 - k_1 \cdot r \qquad \text{(Eq. 4)}$$

Thus, r/c_f as a function of r (Scatchard plot) yields the number of binding sites, n_1, when $r/c_f \to 0$ and the negative slope of the straight line corresponds to the intrinsic association constant k_1. Assuming that $r \neq f(\Delta F_e)$, where ΔF_e is the electrostatic free-energy change, the Scatchard plot yields a curve resulting from interference of the individual curves representing the two types of binding sites. Hence, Eq. 4 can be written

$$\frac{r}{c_f} = \frac{r_1 + r_2}{c_f} = k_1 \cdot n_1 - k_1 \cdot r_1 + k_2 \cdot n_2 - k_2 \cdot r_2 =$$
$$k_1 \cdot n_1 + k_2 \cdot n_2 - [(k_1 - k_2)r_1 + k_2 \cdot r] \qquad \text{(Eq. 5)}$$

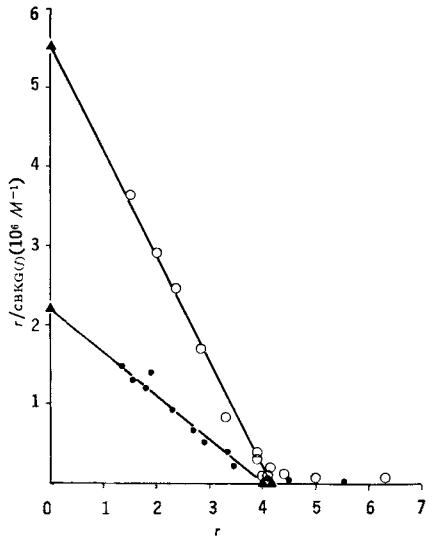

Figure 3—*BKG–BA interaction (pH 7.00). Scatchard plots for primary binding sites. Key: ●, equilibrium dialysis, ionic strength 0.19; and ○, ultracentrifuge sedimentation, ionic strength 0.04. For further details, see* Results.

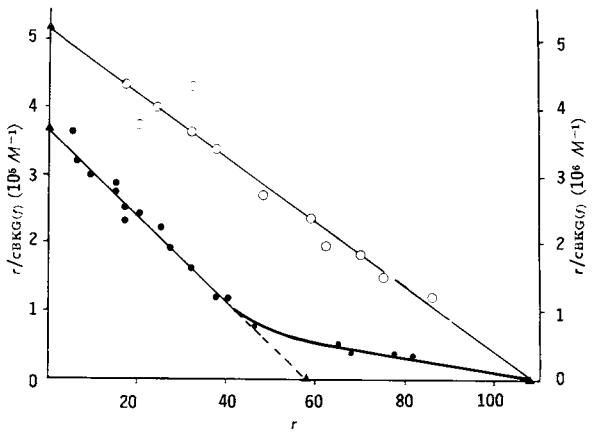

Figure 4—*BKG–BA interaction. Scatchard plots for binding at pH 5.0* (○) *(left scale) and pH 3.5* (●) *(right scale). Ultracentrifuge sedimentation. For further details, see* Results.

Table II—EOS–BA Interaction Showing Binding Parameters by Ultracentrifuge Sedimentation at 21°[a]

pH	Ionic Strength	n_1	n_2	k_1, 10^6 l./mole	k_2, 10^5 l./mole	$\Delta F_1°$, cal./mole	$\Delta F_2°$, cal./mole
7.0	0.04[h]	3.9 ± 0.1	5.8 ± 0.4	5.62 ± 0.22	2.31 ± 0.17	−9077	−7213
7.0	0.19[e]	3.8 ± 0.1	5.6 ± 0.5	9.70 ± 0.51	1.09 ± 0.08	−9324	−6773
5.0	0.24[i]	7.6 ± 0.4	10.6 ± 0.4	0.80 ± 0.04	1.28 ± 0.03	−7938	−6868
3.5	0.24[i]	65 ± 5	0	4.09 ± 0.41	0	−8891	0
3.5	0.25[k]	61 ± 6	0	1.34 ± 0.12	0	−8240	0

[a] For identification of [e], [h], [i], and [k], see Table I.

and in the limit, when r_1, r_2, and $r \rightarrow$ zero,

$$\frac{r}{c_f} \rightarrow k_1 \cdot n_1 + k_2 \cdot n_2 \qquad \text{(Eq. 6)}$$

For $r/c_f \rightarrow 0$,

$$r \rightarrow n_1 + n_2 \qquad \text{(Eq. 7)}$$

From Eq. 5, one obtains the negative slope:

$$-\frac{d(r/c_f)}{dr} = k_2 + (k_1 - k_2)\frac{dr_1}{dr} \qquad \text{(Eq. 8)}$$

For $k_1 \gg k_2$ and low values of r, $dr_1/dr = 1$ as a first approximation; hence the negative slope is $-k_1$, valid for the experimental range $dr_1/dr \simeq 0$, where $d(r/c_f)/dr$ approaches $-k_2$ and r reaches its limiting value of $n_1 + n_2$.

For the determination of the slopes $-k_1$ and $-k_2$, n_1 and n_2, as well as of the y-intercept $k_1n_1 + k_2n_2$ for $r \rightarrow 0$, the authors developed a best-fit computer program which also permitted the calculation of the standard free-energy (free-enthalpy) changes, $\Delta F_1°$ and $\Delta F_2°$, from the obtained intrinsic association constants.

The binding parameters obtained for the BKG–BA interaction at pH 7.0, 5.0, and 3.5 are listed in Table I; the corresponding binding curves are shown in Figs. 3 and 4. In all dialysis and ultracentrifuge experiments, three BKG concentrations were used (4×10^{-5}, 10^{-4}, and 5×10^{-4} M), and the BA concentration was varied within the range 5×10^{-6} to 1.25×10^{-4} M.

EOS–BA—For the characterization of this interaction, spectrophotometry and ultracentrifugation were employed.

Spectrophotometric titrations at 23° of 2.5×10^{-5} M EOS solutions at pH 7.0, 5.0, and 3.5 with 2.5×10^{-5} to 3.1×10^{-7} M BA solutions of corresponding pH values yielded at saturation BA–EOS stoichiometries of 1:3.2, 1:2.1, and 1:0, respectively. Normal and difference spectra demonstrate a red-shift maximum between 532 and 534 mμ and a clear isobestic point at 520–522 mμ (Fig. 5).

The binding parameters, as obtained from ultracentrifuge experiments, are listed in Table II. In these experiments, the EOS concentration was held constant at 2.5×10^{-5} M, whereas the BA concentration was varied in the range 6×10^{-8} to 1.25×10^{-5} M.

IP–BA—Free-enthalpy, enthalpy, and entropy changes of the IP–BA interaction were determined by means of equilibrium dialysis in an IP concentration range (2×10^{-5} to 2×10^{-4} M) which produces 1:1 complex formation; the BA concentration was 2×10^{-5} M. When $r = 1$ (1:1 complexing), Eq. 3 becomes

$$r = \frac{k_1 \cdot c_f}{1 + k_1 \cdot c_f} \qquad \text{(Eq. 9)}$$

or

$$\frac{1}{r} = \frac{1}{c_f \cdot k_1} + 1 \qquad \text{(Eq. 10)}$$

The $1/r$ plotted as a function of $1/c_f$ yields, at 20 and 4°, intercepts of 1.04 ± 0.05 and 0.98 ± 0.07, respectively. The binding parameters and thermodynamic functions are listed in Table III. Analogous experiments with human albumin (HA) yielded an approximately 35% lower association constant.

Binding studies performed in the gravitational field of the ultracentrifuge, with a 13.7 to 360 molar excess of IP and BA concentrations of 10^{-5} and 0.5×10^{-5} M, yield the straight-line binding curve depicted in Fig. 6. The binding parameters calculated according to Eq. 4 are listed in Table IV.

DMI–BA—The interaction of DMI and BA, as studied under the same experimental conditions (21°, pH 7.0, ionic strength I = 0.04), is of a more complex nature. The Scatchard plot yields, for values of r in the range 0–8, a curve with an initially positive slope $d(r/c_f)/dr$ and a maximum at $r \simeq 6$; therefore, the model introduced previously cannot be employed for the DMI–BA interaction. For the interpretation of this mechanism of interaction, an r *versus* c_f plot (Fig. 7) seems to be useful. In the concentration range leading to 1:1 complex formation, the DMI interaction is of the type described for IP.

DISCUSSION

BKG–BA Interactions—Within the limits of experimental error, various methods [equilibrium dialysis, ultracentrifuge sedimentation, and ultrafiltration (27, 28)] yield under identical experimental conditions the same binding parameters such as association constants and number of binding sites (compare Table I). If the intrinsic association constant determined by Rodkey (27) by means of ultrafiltration and that determined in this paper are averaged, the result is $k_1 = 5.45 \times 10^5$ l./mole, with a relative error of 3.5%. In this context, the number of primary binding sites as a function

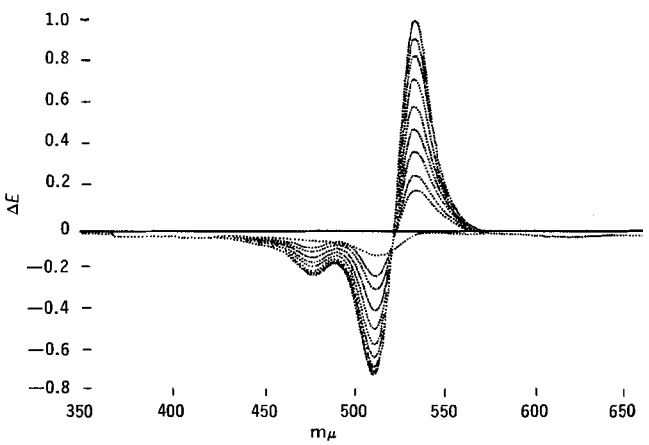

Figure 5—*EOS–BA interaction. Difference spectra by spectrophotometric titrations of EOS with albumin solutions. For further details, see* Results.

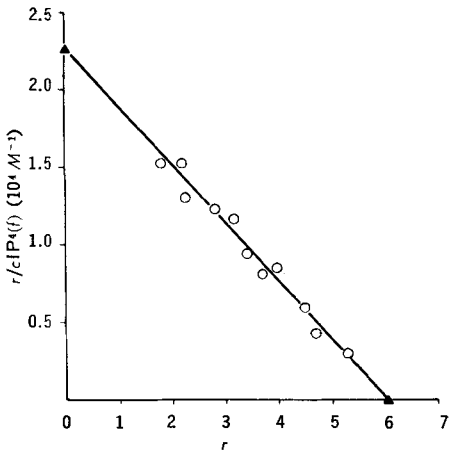

Figure 6—*IP–BA interaction (pH 7.00). Scatchard plot. Ultracentrifuge sedimentation, ionic strength 0.04. For further details, see* Results.

Table III—IP–Albumin Interaction Showing Binding Parameters and Thermodynamic Functions (pH 7.4) by Equilibrium Dialysis[a]

Albumin	Temperature	k_1, 10^3 l./mole	$\Delta F_1°$, cal./mole	$\Delta H_1°$,[b] cal./mole	$\Delta S_1°$,[c] cal. × degree^{-1} × mole^{-1}
Bovine	20°	6.00 ± 0.25	−5063	−5720	−2.2
Bovine	4°	10.60 ± 0.49	−5100		
Human	20°	3.82 ± 0.25	−4800		

[a] For other symbols and the buffer used, see Table I. Ionic strength 0.19. [b] $\Delta H_1°$ = enthalpy change. [c] $\Delta S_1°$ = entropy change.

of pH is of interest. Spectrophotometric titration yielded $n_1 = 3.6$ at pH 7.0. At pH 5.0 and 3.5, the red shift of the difference spectrum has disappeared, but ultracentrifuge experiments yield n_1 values of 58 ± 2 and 108 ± 8. This allows the conclusion that the additional binding sites are chemically different from the ones exhibited at pH 7.0. It can be assumed that the four binding sites observed in the native state of the albumin are lost by unfolding of the protein at low pH. It must be recalled that at pH 7.0, secondary binding sites ($n_2 = 3$ to 4) are also detectable. However, because $k_2 \ll k_1$, n_2 cannot be determined accurately from the experimental data; k_2 is about 5×10^6 l./mole and is thus comparable with the observed intrinsic association constant at pH 3.5, $k_1 = 4.7 \times 10^6$ l./mole.

The albumin molecule is known to undergo a reversible conformation change at pH ≃ 4 (29). Electrostatic interaction forces within the albumin molecule cause an expansion of the molecule to take place, leading to the formation of a species of the so-called *F*-form having greater electrophoretic mobility and higher viscosity (30). In contrast, the *N*-form (native state) has significantly more compact packing. The binding forces for hydrophobic molecules are strongly diminished by an *N–F* transition (30, 31).

At pH 3.5, the binding mechanism is relatively simple: the albumin molecule carries a positive excess charge, and the *N–F* transition has occurred. BKG is present as a univalent anion, so the obtained free-enthalpy change of $\Delta F_1° \simeq -5100$ cal./mole can be attributed to electrostatic interactions. The number of binding sites, $n_1 = 108 \pm 8$, may be accounted for by the basic (cationic) amino acid residues. This binding model (Eq. 3) is confirmed by the straight line in Fig. 4 and by the agreement of the experimentally determined n_1k_1 value (5.15×10^6 l./mole) and the calculated one (5.11×10^6 l./mole).

At pH 5.0, two different binding curves are obtained. Since $k_1 > k_2$, the latter value and thus $\Delta F_2°$ may have been somewhat overestimated (Table I). A more realistic value for $\Delta F_2°$ would be around −3800 cal./mole. It is likely that $\Delta F_1°$ (−4950 cal./mole) represents electrostatic interactions involving the monovalent BKG anion and $\Delta F_2°$ (−3800 cal./mole) those with the bivalent BKG anion. In the BKG–HA system, Rodkey (28) observed a 20% decrease in the association constant at pH 4.8 as compared to pH 3.4. A weak conformational change of the albumin molecule at pH 5.0 appears sufficient for the exposure of the same number of binding sites as is observed in the case of the *N–F* transition. Conformational changes induced by ligand–protein interaction or protein unfolding also should not be excluded.

Table IV—IP–BA Interaction Showing Binding Parameters by Ultracentrifuge Sedimentation at 21°[a]

pH	Ionic Strength	n_1	k_1, 10^3 l./mole	$\Delta F_1°$, cal./mole
7.4	0.04[h]	6.31 ± 0.24	3.59 ± 0.12	−4781
7.0	0.04[h]	6.05 ± 0.19	3.76 ± 0.13	−4808
7.0	0.19[e]	6.12 ± 0.16	6.36 ± 0.41	−5114

[a] For identification of [h] and [e], see Table I.

At pH 7.0, the binding mechanism appears not to be of a solely electrostatic nature. This is not surprising since the albumin molecule, which is in its native state, has a negative excess charge, causing electrostatic repulsion forces with respect to the BKG which exists as the bivalent anion only at pH 7.0. At an ionic strength of 0.19, the negative free-enthalpy change for the primary reaction ($n_1 \simeq 4$) is approximately 4000 cal./mole higher than the $\Delta F_1°$ assumed for the bivalent anion at pH 5.0. However, $-\Delta F_1°$ is increased by about 500 cal./mole through the decrease of the ionic strength by a factor of 5. This confirms the participation of stabilizing electrostatic interaction forces.

In conclusion, the following interpretation of the BKG–BA interaction emerges: (*a*) four primary binding sites predominantly interacting by means of proton donator–acceptor forces (hydrogen bonds), electron donator–acceptor forces, and possibly hydrophobic forces (total $-\Delta F_1° = 4000$ cal./mole), and stabilized further by electrostatic forces ($-\Delta F_1° \simeq 3800$ cal./mole, dependent on ionic strength); and (*b*) three to four secondary binding sites apparently interacting by means of electrostatic forces only ($-\Delta F_2° \simeq 5000$ cal./mole, $k_2 \simeq 5 \times 10^4$ l./mole).

Hydrophobic binding of straight-chain fatty acids by BA, involving stabilizing electrostatic forces, were also observed by Ray *et al.* (32).

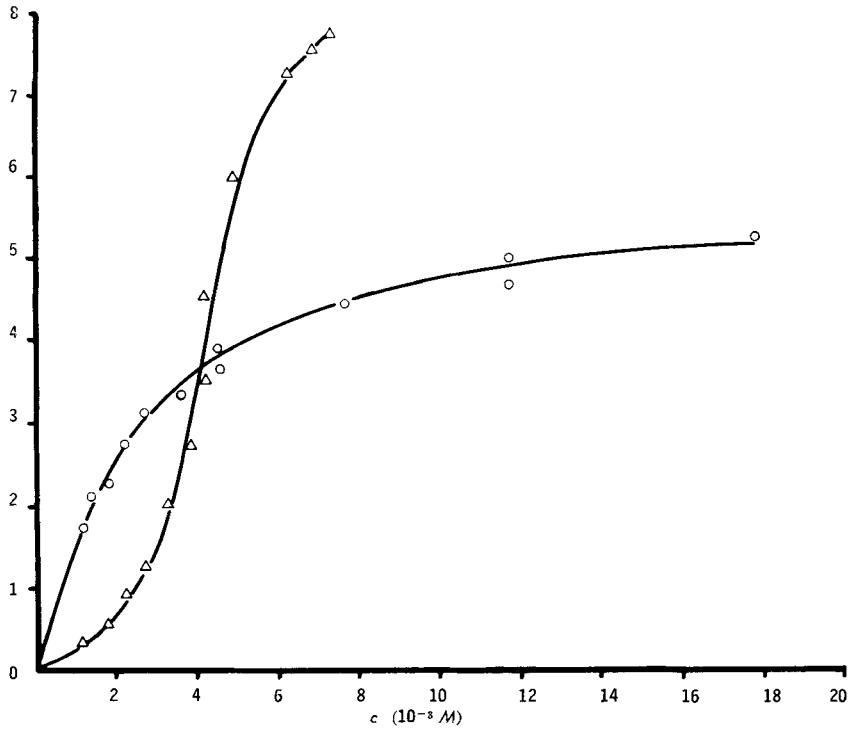

Figure 7—*IP–BA and DMI–BA interactions. Degree of binding* (r) versus *free concentration* (c_f). *Key:* ○, *imipramine*; *and* △, *desipramine. Ultracentrifuge sedimentation, pH 7.0, ionic strength 0.04. For further details, see* Results.

EOS–BA Interactions—At pH 3.5, the simple binding model with one type of binding site is again confirmed. It also can be assumed that electrostatic forces predominate because of the unfolding of the albumin molecule, its positive excess charge, and the charge distribution of the ligand. An increase of the ionic strength by a factor of about 3 produces a decrease of the free-enthalpy change by about 700 cal./mole (Table II), but the number of binding sites remains unchanged ($n_1 \simeq 60$) and is considerably smaller in comparison to BKG.

At pH 7.0, the ionic strength dependence of the free-enthalpy change is opposite for the two types of binding sites. The primary binding sites ($n_1 \simeq 4$) are likely to interact by means of van der Waals' forces, since an increased electrolyte concentration reduces the dielectric constant of water and thus increases the association constant (by a factor of about 2). Although in a strictly physical sense the van der Waals forces apply only to dispersion forces, the authors employ the term in a broader sense according to Martin (33), whereby it should be noted that dipole–dipole interactions are stabilized by energy effects and true dispersion forces by entropy effects. The free-enthalpy change involving the secondary binding sites ($n_2 \simeq 6$) is approximately 2000 cal./mole smaller than $-\Delta F_1°$. However, in this case, electrostatic forces appear to predominate, since an increase of the ionic strength by a factor of 5 reduces the $-\Delta F_2°$ by about 450 cal./mole (Table II).

Spectrophotometric titrations at pH 7.0 and 5.0 yielded binding stoichiometries of BA–EOS = 1:3.2 and 1:2.1, respectively.

The binding mechanism at pH 5.0 appears to be more specific than for BKG, since $n_1 + n_2$ is smaller by about 80 binding sites. An accurate interpretation of the binding mechanism at this pH, which is the approximate isoelectric point of albumin, is again difficult. Despite comparable ionic strengths, $-\Delta F_1°$ is about 1400 cal./mole lower than at pH 7.0.

Finally, from the interaction data at hand, no structural relationships between ligand and protein can be derived. A possible participation of ϵ-amino groups of lysine is indicated by preliminary experiments showing that the majority of these groups are blocked for dinitrofluorobenzene after binding of BKG or EOS.

IP–BA and DMI–BA Interactions—From the temperature dependence, the resulting thermodynamic functions, and the ionic strength dependence of the IP–BA binding reaction in the 1:1 complexing range, it can be concluded that participation of van der Waals' forces is predominant. From the negative enthalpy change of 5700 cal./mole, it can be concluded that the forces under consideration are energetically stabilized, probably by dipole–dipole interactions. Hydrophobic forces cannot be excluded, since the entropy function ($\Delta S_i° = -2.2$ cal. $\times$ degree^{-1} $\times$ mole^{-1}) is very small. However, it is certain that they do not constitute the main interaction forces in contrast with sulfonamide–albumin binding, where Clausen (34) measured positive ΔS values of 20–30 cal. $\times$ degree^{-1} $\times$ mole^{-1}. In the case of IP, a decrease of the ionic strength by a factor of 5 produces at constant temperature a reduction of the intrinsic association constant by almost 50% and a corresponding reduction of the free-enthalpy change by about 300 cal./mole. Both equilibrium dialysis and ultracentrifuge sedimentation yield, under like conditions, the same binding parameters (Tables III and IV). The obtained number of binding sites averages $n_1 = 6.2 \pm 0.2$. The reason for the somewhat weaker binding tendency of human albumin may lay in the higher degree of purity of the bovine preparation employed (35).

UV difference spectra (performed with a Cary 14 recording spectrophotometer) at various degrees of binding (r_i) demonstrate marked red shifts at 21° within both the 220–235 and 260–310 mμ wavelength bands. According to Wetlaufer (36), red shifts are commonly associated with aromatic ($\pi \rightarrow \pi^*$) and peptide transitions. According to other authors (32, 37, 38), these red shifts are produced by tyrosine side-chain chromophores. This short wavelength red shift and its sign are typical of protein complexes in which the higher tryptophan-associated sites are not engaged. These spectroscopic data are also obtained by the binding to albumin of long-chain fatty acid anions (38). On the basis of the number of binding sites ($n_1 \simeq 6$), it can be assumed that tyrosine residues participate directly or indirectly in the IP–BA interaction.

Herskovits *et al.* (39–41) studied, with the aid of the solvent perturbation technique, the location of tyrosyl and tryptophyl residues in bovine serum albumin. Their results, at pH 6.8, show that about 70% of the 18 to 21 tyrosyl residues appear to be buried in the folds of the native protein, while the remaining tyrosyl groups are accessible to perturbants with molecule diameters less than 5.2 Å. The two tryptophyl residues present in the protein are found to be nearly fully exposed to perturbants with less than 4.4 A diameter, while about 50% exposure is observed with perturbants having greater than 5.2 Å diameter.

The data obtained in the case of the DMI–BA interaction indicate the involvement of a far more complicated mechanism than with IP–BA. The postulated binding models fail to explain the data. The *r versus* c_f plot of DMI (Fig. 7) yields a sigmoidal curve. In contrast to IP, UV difference spectra show blue shifts in the long wavelength and, particularly, in the short wavelength regions. The sigmoidal binding curve and the UV spectral properties allow the following interpretations for the DMI–BA complex. (*a*) Tyrosyl or tryptophyl residues are directly or indirectly involved. (*b*) A primary interaction of DMI and BA induces a change of the tertiary structure, *e.g.*, by a certain degree of unfolding, or a conformational change presumably in secondary segments of the polypeptide chain. This is suggested by the variation in reactivity of the binding sites involved. The binding mechanism is thus governed by cooperative phenomena. (*c*) The number of binding sites amounts to at least eight (Fig. 7).

Finally, it should be noted that the binding parameters obtained by different methods need not necessarily agree. Thus, the fraction calculated to be bound by gel filtration was one-third that found with equilibrium dialysis under identical experimental conditions (42). Such a disparity is determined by structural characteristics of ligands and gel phase. A combination of several methods is, therefore, advisable to avoid false conclusions. Supplementary NMR data on IP–BA and DMI–BA interactions are currently being collected and will be published.

REFERENCES

(1) W. Kauzmann, *Advan. Protein Chem.*, **14,** 1(1963).

(2) W. Kauzmann, "Quantum Chemistry," Academic, New York, N.Y., 1967.

(3) M. C. Meyer and D. E. Guttman, *J. Pharm. Sci.*, **57,** 895 (1968).

(4) H. J. Weder and M. H. Bickel, *ibid.*, **59,** 1505(1970).

(5) A. R. Peacocke and J. N. H. Skerrett, *Trans. Faraday Soc.*, **52,** 261(1956).

(6) H. A. Benesi and J. H. Hildebrand, *J. Amer. Chem. Soc.*, **71,** 2703(1949).

(7) G. G. Hammes and P. R. Schimmel, *ibid.*, **87,** 4665(1965).

(8) F. Karush and M. Sonnenberg, *ibid.*, **71,** 1369(1949).

(9) T. Higuchi, R. Kuramoto, L. Kennon, T. L. Glagon, and A. Polk, *J. Amer. Pharm. Ass., Sci. Ed.*, **43,** 646(1954).

(10) G. Scatchard, I. H. Scheinberg, and S. H. Armstrong, *J. Amer. Chem. Soc.*, **72,** 535(1950).

(11) I. M. Klotz, F. M. Walker, and R. B. Pivan, *ibid.*, **68,** 1486 (1946).

(12) P. Spring, *Arzneim.-Forsch.*, **16,** 346(1966).

(13) R. M. Rosenberg and I. M. Klotz, in "A Laboratory Manual of Analytical Methods of Protein Chemistry," vol. 2, P. Alexander and R. J. Block, Eds., Pergamon, New York, N. Y., 1960, p. 131.

(14) W. Scholtan, *Makromol. Chem.*, **54,** 24(1962).

(15) G. Jürgensen, Ph. D. thesis, ETH, Zürich, Switzerland, 1966.

(16) I. Z. Steinberg and H. K. Schachman, *Biochemistry*, **5,** 3728(1966).

(17) H. K. Schachman, "Ultracentrifugation in Biochemistry," Academic, New York, N. Y., 1959, p. 169.

(18) G. Scatchard, *Ann. N. Y. Acad. Sci.*, **51,** 660(1949).

(19) J. T. Edsall and J. Wyman, "Biophysical Chemistry," vol. 1, Academic, New York, N. Y., 1960.

(20) G. A. J. van Os, *Arzneim.-Forsch.*, **16,** 1428(1966).

(21) H. E. Hard, *Bull. Math. Biophys.*, **27,** 87(1965).

(22) H. A. Rosenthal, *Anal. Biochem.*, **20,** 525(1967).

(23) C. Hansch, K. Kiens, and G. L. Lawrence, *J. Amer. Chem. Soc.*, **87,** 5770(1965).

(24) R. Franke, *Biochim. Biophys. Acta*, **160,** 378(1968).

(25) D. M. Crothers, *Biopolymers*, **6,** 575(1968).

(26) L. W. Nichol, W. J. H. Jackson, and D. J. Winzor, *Biochemistry*, **8,** 2449(1967).

(27) F. L. Rodkey, *Arch. Biochem. Biophys.*, **94,** 526(1961).

(28) *Ibid.*, **108,** 510(1964).

(29) J. F. Foster, in "The Plasma Proteins," vol. 1, F. W. Putnam, Ed., Academic, New York, N. Y., 1960.
(30) A. Wishnia and T. Pinder, *Biochemistry*, **3**, 1377(1964).
(31) D. E. Guttman and A. E. Gadzala, *J. Pharm. Sci.*, **54**, 742 (1965).
(32) A. Ray, J. A. Reynolds, H. Polet, and J. Steinhardt, *Biochemistry*, **5**, 2606(1966).
(33) A. N. Martin, "Physical Pharmacy," Lea & Febiger, Philadelphia, Pa., 1960.
(34) J. Clausen, *J. Pharmacol. Exp. Ther.*, **153**, 167(1966).
(35) H. B. Bull and K. Breese, *Arch. Biochem. Biophys.*, **120**, 303(1967).
(36) D. B. Wetlaufer, *Advan. Protein Chem.*, **17**, 303(1962).
(37) H. Polet and J. Steinhardt, *Biochemistry*, **7**, 1348(1968).
(38) J. A. Reynolds, S. Herbert, and J. Steinhardt, *ibid.*, **7**, 1357 (1968).
(39) T. T. Herskovits and M. Laskowski, *J. Biol. Chem.*, **237**, 2481(1962).
(40) T. T. Herskovits and M. Sorensen, *Biochemistry*, **7**, 2523 (1968).
(41) *Ibid.*, **7**, 2533(1968).
(42) H. J. Weder and R. Gauch, unpublished results.

ACKNOWLEDGMENTS AND ADDRESSES

Received November 11, 1969, from the *Medizinisch-chemisches Institut, University of Berne, Berne, Switzerland.*
Accepted for publication April 14, 1970.
* Present address: Institute of Molecular Biology and Biophysics, Federal Institute of Technology, Zurich, Switzerland.

Pharmacokinetic Model for Chlordiazepoxide·HCl in the Dog

S. A. KAPLAN, M. LEWIS, M. A. SCHWARTZ, E. POSTMA, S. COTLER, C. W. ABRUZZO, T. L. LEE, and R. E. WEINFELD

Abstract □ A six-compartment open-system model is presented to elucidate the physiological disposition of chlordiazepoxide and its two pharmacologically active biotransformation products, Ro 5-0883/1 and Ro 5-2092, in the dog following the intravenous administration of 10 mg./kg. chlordiazepoxide·HCl. The pharmacokinetic parameters used in the model were obtained by administering each of the three compounds separately. Excellent agreement was obtained between the plasma levels of intact drug, Ro 5-0883/1, and Ro 5-2092 found after administration of chlordiazepoxide·HCl and the calculated levels of each generated from the model. The main features of chlordiazepoxide disposition were: (*a*) its complete biotransformation to Ro 5-0883/1; (*b*) elimination of Ro 5-0883/1 almost entirely by biotransformation with up to 50% proceeding to Ro 5-2092 by oxidative deamination; and (*c*) elimination of Ro 5-2092 by urinary excretion and further biotransformation.

Keyphrases □ Chlordiazepoxide·HCl and metabolites, disposition—pharmacokinetic model □ Biotransformation, dogs—chlordiazepoxide·HCl □ Plasma levels—chlordiazepoxide and metabolites □ Urinary excretion—chlordiazepoxide and metabolites □ TLC—separation □ Fluorometry—analysis

Chlordiazepoxide[1] (7-chloro-2-methylamino-5-phenyl-3*H*-1,4-benzodiazepine 4-oxide) is extensively used in the treatment of anxiety states and other psychic disorders (1, 2). Chlordiazepoxide has been shown (3–5) to be biotransformed in dog and man to the *N*-demethyl chlordiazepoxide (Ro 5-0883/1), which undergoes further deamination to form the "lactam" (Ro 5-2092). The structure of chlordiazepoxide together with those of the two biotransformation products, both of which are pharmacologically active (2, 6, 7), is presented in Scheme I.

This study reports the development of a pharmacokinetic model to describe the physiological disposition of chlordiazepoxide, Ro 5-0883/1, and Ro 5-2092 following the intravenous administration of chlordiazepoxide·HCl to dogs. To elucidate an appropriate pharmacokinetic model, each of the three compounds was separately administered intravenously to two dogs. The pharmacokinetic parameters thus obtained for each compound were used to establish the model for the disposition of chlordiazepoxide·HCl.

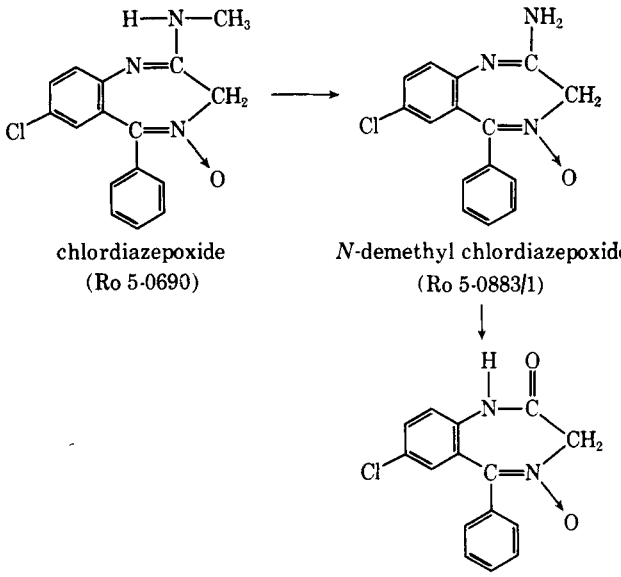

Scheme I

EXPERIMENTAL

Protocol—Two male dogs, weighing 10.5 and 13.0 kg., each received single 10-mg./kg. i.v. doses of chlordiazepoxide·HCl, Ro

[1] Chlordiazepoxide·HCl is the active ingredient in Librium marketed by Hoffmann-La Roche Inc., Nutley, N. J.